UNDERSTANDING OPPORTUNITIES FOR EFFICIENCY IN SINGLE-IMAGE SUPER RESOLUTION NETWORKS

Anonymous authors
Paper under double-blind review

ABSTRACT

A successful application of convolutional architectures is to increase the resolution of single low-resolution images – a image restoration task called super-resolution (SR). Naturally, SR is of value to resource constrained devices like mobile phones, electronic photograph frames and televisions to enhance image quality. However, SR demands perhaps the most extreme amounts of memory and compute operations of any mainstream vision task known today, preventing SR from being deployed to devices that require them. In this paper, we perform a early systematic study of system resource efficiency for SR, within the context of a variety of architectural and low-precision approaches originally developed for discriminative neural networks. We present a rich set of insights, representative SR architectures, and efficiency trade-offs; for example, the prioritization of ways to compress models to reach a specific memory and computation target and techniques to compact SR models so that they are suitable for DSPs and FPGAs. As a result of doing so, we manage to achieve better and comparable performance with previous models in the existing literature, highlighting the practicality of using existing efficiency techniques in SR tasks. Collectively, we believe these results provides the foundation for further research into the little explored area of resource efficiency for SR.

1 INTRODUCTION

Rapid progress has been made in the development of convolutional networks (Dong et al., 2015) that are capable of taking a low-resolution image and producing an image with a significant increase in resolution. This image restoration task is referred to as super-resolution (SR) and has many potential applications in devices with limited memory and compute capacity. The fundamental problem however is that the state-of-the-art networks (Lim et al., 2017; Zhang et al., 2018; Zhang et al., 2018) consist of thousands of layers and are some of the most resource intensive networks currently known. Furthermore, due to the spatial dimensions of feature maps needed to maintain or up-scale the input, the number of operations are counted in the billions as opposed to millions in models for discriminative tasks. As a result, there is a need for a general systematic approach to improve the efficiency of SR models.

The challenge of the system resource requirements for deep learning models for tasks other than SR have been carefully studied in previous works (Zhang et al., 2017b; Howard et al., 2017; Ma et al., 2018; Sandler et al., 2018), achieving massive gains in size and compute with little to no loss in performance. These reductions are achieved with a wide variety of methods being developed grounded in primarily architecture-level changes and techniques grounded in the use of low precision and quantized model parameters. However, how these efficiency methods behave when applied within SR have not yet been studied in significant depth, with very few results published in the literature. Extrapolating from prior results for other tasks is problematic given that predominantly existing studies are applied to discriminative tasks with substantially different architectures and operations. Due to the up-sampling structure of SR models, these efficiency methods may therefore produce potentially stronger side-effects to image distortion.

In this paper, we detail a systematic study that seeks to bridge current understanding in SR and known approaches for scaling down the consumption of system resources by deep models. By examining the impact on image distortion quality when performing various efficiency techniques, we provide the following new insights:

- The effectiveness of low rank tensor decomposition and other convolution approximations, which are comparable and successful in discriminative tasks, can vary considerably in SR. (See section 4.1).
- Unlike image discriminative networks, SR networks suffer from a worse trade-off between efficiency and performance as more layers are compressed. (See section 4.2)
- The practicality of adopting compression techniques for other tasks to SR as our best models are better or comparable to existing literature. For instance, our best model achieves significantly better performance and 6x less compute than MemNet (Tai et al., 2017b) and VDSR (Kim et al., 2015b). Additionally, it also performs better and is 4.1x-5.8x smaller than SRMDNF (Zhang et al., 2017a). (See section 4.3)
- Successful quantization techniques used in image discriminative tasks are equally successful in SR. (See section 5)

2 RELATED WORK

We focus on using neural networks for SR as they have shown to achieve superior performance against previous traditional approaches (Timofte et al., 2013; Kim & Kwon, 2010; Chang et al., 2004). An SR image can either be evaluated using standard image distortion metrics, such as PSNR, SSIM (Wang et al., 2004) and IFC (Sheikh et al., 2005), or using perception metrics, such as Ma et al. (2016), NIQE (Mittal et al., 2013), and BRISQUE (Mittal et al., 2012). Blau & Michaeli (2017) provided theoretical backups on the trade-off between image distortion and perception.

Distortion SR: In the distortion line of work, models favour pixel-to-pixel comparisons and are usually trained on either the L1 or L2 (MSE) loss. These models have been known to produce more visually pleasing outcomes on structural images Blau et al. (2018) than perceptual SR models. Dong et al. (2015) first proposed using convolutional networks for SR, leading to a surge in using neural networks for SR. These networks differ in their building blocks for feature extraction and up-sampling. For instance, Dong et al. (2016) proposed a faster convolutional network by taking the down-sampled low-resolution image as an input. Other variations include using more layers (Kim et al., 2015b), recursive layers (Kim et al., 2015a; Tai et al., 2017a), memory blocks (Tai et al., 2017b; Ahn et al., 2018), DenseNet (Huang et al., 2016) blocks (Tong et al., 2017), residual (He et al., 2015) blocks (Ledig et al., 2016; Lim et al., 2017; Kim & Lee, 2018), and multiple-image degradations (Zhang et al., 2017a). Additionally, more recent models use attention (Bahdanau et al., 2014) mechanisms (Liu et al., 2018; Zhang et al., 2018), back-projection (Haris et al., 2018; Navarrete Michelini et al., 2018), and other non-conventional non-linear layers (Choi & Kim, 2017; Gu et al., 2018).

Perceptual SR: Perceptual SR models, on the other hand, are better at reconstructing unstructured details with high perceptual quality (Blau et al., 2018). These models usually adopt popular models for image distortion and train them using a variety of different loss functions, such as the perceptual loss (Johnson et al., 2016), contextual loss (Mechrez et al., 2018b), adversarial loss (Goodfellow et al., 2014), and the Gram loss (Gatys et al., 2015). For instance, Choi et al. (2018) adopted EUSR Kim & Lee (2018) and Ledig et al. (2016); Wang et al. (2018); Mechrez et al. (2018a) adopted SRResNet (Ledig et al., 2016) by making slight architecture changes and replacing the objective. Although these perceptual models are able to generate more visually pleasing results on certain images, they do not seem to work well as inputs for image classification (Jaffe et al., 2017).

Efficient SR: As models in both tracks are resource-intensive, the recent PIRM 2018 Challenge for mobile (Ignatov et al., 2018) presented a range of high efficiency models that were designed to run faster and perform better than SRCNN (Dong et al., 2015). These models are complementary to our work and can follow our best practices to achieve greater efficiency gains. A work closely related to our work is done by Ahn et al. (2018) who systemically investigate the impact of using grouped convolutions. Due to the massive design space caused by the variability of training and evaluating these models, we focus on the trade-offs between performance measured by the image distortion metrics and efficiency and leave the rest as future work.

3 SYSTEMATIC STUDY OF LOW-RESOURCE SUPER RESOLUTION NETWORKS

The key step in our work is to build understanding towards building resource-efficient architectures for super-resolution. While there is a lot of understanding of how these efficiency-saving techniques work in classification problems, there is a lack of experimental studies and systematic approaches to understand their practicality in super-resolution. To our knowledge, this is the first systematic study of wide range efficiency methods on super-resolution.

We measure performances using PSNR and SSIM (Wang et al., 2004) and measure efficiency of memory and compute using the number of parameters and the number of multiply-add operations (Mult-Adds), both of which dictate which platform these models can run on. However, these metrics alone do not reflect the trade-off between performance and efficiency. Therefore, we introduce two new metrics that measures the number of Giga Mult-Adds saved and the number of parameters saved for every 0.01dB PSNR loss in the test sets: Set5 (Bevilacqua et al., 2012), Set14 (Yang et al., 2010), B100 (Martin et al., 2001), and Urban100 (Huang et al., 2015). These metrics are calculated by taking the difference between the compressed model and the uncompressed model. All Mult-Adds are calculated by upscaling to a 720p image.

We decide to use RCAN Zhang et al. (2018) as our baseline model as it proves to be the state-of-the-art and has the best performance in the image distortion metrics at the time of writing. We take its simplest building block and build a shallower network and use that as a basis for exploring the use of a variety of techniques.

Implementation Details: We train our models in section 4 and section 5.1 in the same manner as that of EDSR Lim et al. (2017). In particular, we use 48×48 RGB patches of LR images from the DIV2K dataset Timofte et al. (2017). We augment the training data with random horizontal flips and 90 degree rotations and pre-process them by subtracting the mean RGB value of the DIV2K dataset. Our model is trained using the ADAM Kingma & Ba (2014) optimizer with hyper-parameters $\beta_1 = 0.9, \beta_2 = 0.999$, and $\epsilon = 10^{-8}$. The mini-batch size is 16, learning rate begins with $1e-4$ and is halved at 200 epochs, and the model is trained for 300 epochs using L1 loss. We train x2 models from scratch and use them as pre-trained models to train x3 and x4 models for faster convergence. Lastly, for ternary quantization in section 5.2, we further train the model with quantization enabled in each forward pass for 40 epochs, starting at a learning rate of $5e-5$, and then fix the quantized ternary weights and further train for another 10 epochs at a learning rate of $2.5e-5$.

4 EFFICIENT NETWORK ARCHITECTURES FOR SUPER RESOLUTION

We begin our evaluation by conducting a series of experiments: (i) we explore the effects of applying different resource-efficient architectures to our baseline model (section 4.1), (ii) we consider two best techniques and present trade-off solutions while applying them to different parts of our baseline model (section 4.2), (iii) and lastly, we compare our best results with previous SR architectures (section 4.3).

4.1 EFFECTS OF VARIOUS RESOURCE-EFFICIENT TECHNIQUES

Motivation: Resource-efficient architectures use various low rank tensor decomposition and other convolutional approximation techniques, which is agnostic and is not specifically designed for any particular task, to build fast and accurate image discriminative models. We first develop an initial understanding of the trade-off solution by replacing and modifying 3x3 convolution layer blocks in the baseline model.

Approach: We explore the use of known techniques such as the bottleneck design, separable/grouped convolutions, and channel shuffling. We take the feature extraction unit from resource-efficient architectures and remove all batch normalisation layers as they were previously shown to reduce performance and increase GPU memory usage (Lim et al., 2017). For our first set of experiments, we replace all 3x3 convolution layers in the residual groups of our baseline model.

bl: Our baseline model from RCAN (Zhang et al., 2018). We reduce the number of residual groups (RG) from 10 to 2 and the number of residual channel attention block (RCAB) in each RG from 20 to 5. We use a feature map size of 64. Making the network shallower and small in parameters allow us to clearly understand each architectural changes as opposed to having a deep network which may cause other effects and interplay.

blrn(r): We adopt the residual bottleneck design from ResNet (He et al., 2015) with a reduction factor of r. Specifically, a 1x1 convolution is used to compress information among channels by a reduction factor, resulting in a cheaper 3x3 convolution. Another 1x1 convolution is then used to recover the dimension of the output channel and a skip connection is used to pass on information that may have been lost.

blrxn(r,g): We replace the 3x3 convolution in *blrn* to a 3x3 grouped convolution, forming a block that is similar to that of ResNeXt (Xie et al., 2016) with an additional group size of g. Computation cost is further reduced by the use of grouped convolutions (Krizhevsky et al., 2012).

blm1: In order to further improve efficiency of the 3x3 grouped convolution, we can maximise the group size, forming a convolution that is known as depthwise convolution. Following this idea, we adopt the MobileNet v1 (Howard et al., 2017) unit which uses depthwise separable convolutions, each consist of a 3x3 depthwise convolution followed by a 1x1 convolution, also known as a pointwise convolution.

bleff(r): We can further approximate the 3x3 depthwise convolution by using a 1x3 and a 3x1 depthwise convolution, a technique that is used in EffNet (Freeman et al., 2018). We adopt the unit from EffNet by removing the pooling layers.

bls1(r, g): We group both 3x3 and 1x1 convolutions and added channel shuffling in order to improve the information flow among channels. In order to test the effects of channel shuffling, we adopt the ShuffleNet v1 (Zhang et al., 2017b) unit.

blclc(g1, g2): Channel shuffle is also used in Clcnet (Zhang, 2017) to further improve efficiency of *blm1*. In order to maximise efficiency from our adoption of ClcNet units, we follow the group size guidelines recommended by the authors for both the group sizes of the 3x3 (*g1*) and 1x1 (*g2*) grouped convolution.

bls2: Apart from using grouped convolutions, Ma et al. (2018) proposed splitting the flow into two, which is termed as channel splitting, and performing convolution on only half of the input channels in each unit at each pass. Channel shuffle is then used to enable information flow between both branches.

blm2(e): Inverted residuals can be used to enable skip connections directly on the bottleneck layers. Therefore, we adopt the MobileNet v2 (Sandler et al., 2018) unit in our experiments

Table 1: Quantitative results of applying resource-efficient techniques. **bold**/*italics* indicates best/second-best trade-off.

Scale	Model	Params (K)	Mult-Adds (G)	Set5 PSNR/SSIM	Set14 PSNR/SSIM	B100 PSNR/SSIM	Urban100 PSNR/SSIM	Mult-Add Saved (G)	Params Saved (K)
	bl	1006	231.2	37.86/0.9600	33.39/0.9159	32.06/0.8982	31.74/0.9248	-	-
	blrn(r=2)	464	106.5	37.61/0.9591	33.18/0.9137	31.90/0.8961	31.09/0.9173	**0.9819**	**4.27**
	blm1	265	60.7	37.45/0.9586	33.00/0.9122	31.79/0.8948	30.65/0.9128	*0.7894*	*3.43*
	blrxn(r=2, g=4)	305	69.9	37.45/0.9585	33.01/0.9123	31.80/0.8948	30.71/0.9131	0.7755	3.37
	blrn(r=4)	258	59	37.42/0.9583	32.96/0.9120	31.76/0.8943	30.66/0.9123	0.7653	3.32
2×	blclc(g1=32, g2=2)	232	52.9	37.40/0.9581	32.94/0.9118	31.73/0.8939	30.53/0.9108	0.7278	3.16
	bls2	211	48.4	37.37/0.9580	32.96/0.9117	31.71/0.8936	30.49/0.9102	0.7254	3.15
	bleff(r=2)	257	58.7	37.33/0.9580	32.94/0.9114	31.71/0.8936	30.41/0.9098	0.6485	2.82
	blm2(e=2)	561	128.9	37.43/0.9586	33.08/0.9130	31.81/0.8949	30.77/0.9138	0.5219	2.27
	bls1(r=2, g=4)	188	42.9	37.06/0.9568	32.74/0.9096	31.52/0.8912	29.94/0.9031	0.4968	2.16
	blm2(e=3)	763	175.4	37.56/0.9589	33.11/0.9133	31.86/0.8954	30.93/0.9155	0.3509	1.53

Results: Our results in Table 1 show that techniques that result in a better trade-off between memory and performance will have a better trade-off between compute and performance. [1]. Overall, the use of bottlenecks alone (*blrn*) result in the best trade-offs followed by the use of separable/grouped convolutions.

Reducing the number of features to accommodate inverted bottlenecks (*blm2*) severely impact the performance and thus we omit the results from the table. We speculate that doing so would result in insufficient features at the up-sampling layer to fully capture the up-sampled image representation. Thus, we use the same number of feature maps as our bottleneck. Although the use of inverted

[1]Results for 3x and 4x upscaling show similar performance and efficiency trade-offs

residuals in our experiments seem worse off, it may perform better on models that use a larger feature size or multiple smaller up-sampling layers.

Lastly, the use of 1x1 grouped convolution or channel splitting with channel shuffling further reduces the evaluation metric. Although doing so can drastically reduce size, the trade-off does not seem to justify its advantages. Therefore, we recommend using bottlenecks for building resource-efficient SR architectures. If the budget for memory and efficiency is tight, we recommend the use of depthwise separable convolutions instead.

In image discriminative tasks, the proposed architecture changes are comparable in terms of efficiency and accuracy trade-offs. In our work, we show that the sole use of low rank tensor decomposition (bottleneck architectures) provide the best trade-offs, followed by the use of separable/grouped convolutions and the use of both channel splitting and shuffling.

4.2 Effects of architectural layers between the input and output layer

Motivation: Bhattacharya & Lane (2016) and Kim et al. (2015c) have shown that it is possible in image classification to maintain a similar or slight drop in performance by decomposing tensors of known models. However, our models suffer a significant drop in performance. (Table 1). Therefore, in order to further understand the extent of their applicability in SR, we apply the top two best techniques, which are bottleneck reduction (*blrn*) and depthwise separable convolutions (*blm1*), on various different parts of our baseline model.

Approach: Our preliminary experiments with applying some of these techniques on the first and last convolution layer led to worse trade-offs. Therefore, we apply our techniques between them. We replace the sub-pixel convolution upsampling layer to the enhanced upscaling module (EUM) as proposed by Kim & Lee (2018) to allow the use of skip connections. Using EUM leads to an increase in performance at a slight cost of both memory and compute. Thus, in order to maintain the memory cost, we use recursion, forming the enhanced recursive upscaling module (ERUM) shown in figure 1. The number of ERUMs is the same as the scaling factor and each ERUM recurses twice or thrice for x2, x4 or x3 scales respectively. Experiments that use ERUMs for up-sampling are indicated with a postfix *-e*. We calculate our trade-off metrics based on our baseline model with ERUM as its up-sampling layer instead *bl-e*. We modify all 3x3 convolution layers as such:

rb: Changes are made in residual blocks/modules.

rg: Changes are made in residual groups, therefore including those in *rb*. (Experiments in section 4.1 are done in this setting.)

rg+u: Changes are made in both *rg* and the up-sampling layers (ERUMs).

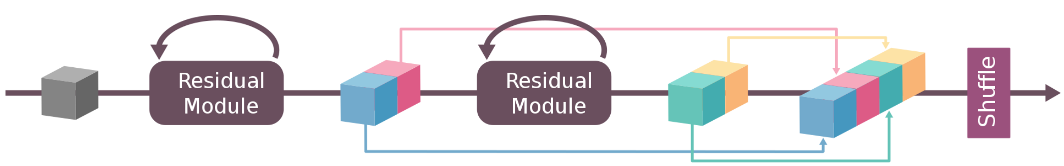

Figure 1: Our proposed ERUM for image upscaling.

Results: Our results in Table 2 reinforce our findings in section 4.1 that the adoption of bottleneck reduction alone leads to the best trade-offs, followed by the use of group convolutions. Therefore, we recommend taking gradual steps to compress the model. For instance, we suggest gradually changing convolutions to use bottleneck reduction, avoiding the up-sampling, first, and last convolutions until a budget is reached. If further compression is needed, we suggest changes to the up-sampling layer or the use of group convolutions.

4.3 Comparisons with previous SR models

We take our derived best models based on different budgets from our first two experiments (See section 4.1 & 4.2) and compare them with the existing literature, which is shown in Table 3. For fair comparisons, we omit models that are way bigger by several magnitudes as their performances are much better. Likewise, we exclude models that are way smaller as their performance are much

Table 2: Quantitative results of applying techniques on different parts of the model. We took the best three derived models given three different budgets and compared them with previous models in Table 3 **bold**/*italics* indicates best/second-best trade-off.

Scale	Model [Changes]	Params (K)	Mult-Adds (G)	Set5 PSNR/SSIM	Set14 PSNR/SSIM	B100 PSNR/SSIM	Urban100 PSNR/SSIM	Mult-Add Saved (G)	Params Saved (K)
2×	bl-e	1006	265.3	37.92/0.9602	33.43/0.9162	32.09/0.8988	31.83/0.9256	-	-
	blrn-e(r=2)[rb]	535	156.8	37.75/0.9596	33.30/0.9153	32.00/0.8973	31.48/0.9218	**1.4662**	**6.3649**
	blm1-e[rb]	363	117	37.65/0.9592	33.19/0.9143	31.92/0.8964	31.13/0.9181	*1.0746*	*4.6594*
	blm1-e[rg]	265	94.7	37.59/0.9590	33.12/0.9132	31.87/0.8959	30.91/0.9158	0.9584	4.1629
	blrn-e(r=2)[rg]	464	140.5	37.64/0.9592	33.20/0.9142	31.93/0.8967	31.18/0.9185	0.9455	4.1061
	blrn-e(r=2)[rg+u]	370	97.1	37.56/0.9589	33.10/0.9131	31.86/0.8954	30.99/0.9164	0.9557	3.6136
	blm1-e[rg+u]	137	35.4	37.35/0.9580	32.94/0.9117	31.72/0.8939	30.45/0.9103	0.8181	3.0925
3×	bl-e	1080	156.3	34.35/0.9269	30.29/0.8415	29.06/0.8046	28.13/0.8521	-	-
	blrn-e(r=2)[rb]	609	108.1	34.19/0.9257	30.18/0.8394	29.00/0.8026	27.89/0.8469	**0.8456**	**8.2632**
	blm1-e[rb]	437	90.5	34.09/0.9249	30.13/0.8379	28.95/0.8015	27.69/0.8419	0.6784	*6.6289*
	blrn-e(r=2)[rg+u]	397	57.6	33.97/0.9236	30.04/0.8362	28.89/0.7997	27.50/0.8376	*0.6902*	4.7762
	blrn-e(r=2)[rg]	538	100.9	34.13/0.9251	30.14/0.8380	28.97/0.8016	27.72/0.8421	0.6368	6.2299
	blm1-e[rg]	339	80.6	34.08/0.9244	30.03/0.8356	28.92/0.8005	27.55/0.8386	0.6056	5.928
	blm1-e[rg+u]	146	21.4	33.73/0.9221	29.83/0.8320	28.78/0.7970	27.10/0.8283	0.5644	3.9079
4×	bl-e	1154	135.5	32.08/0.8942	28.58/0.7815	27.56/0.7360	26.16/0.7872	-	-
	blrn-e(r=2)[rb]	683	108.3	32.10/0.8938	28.51/0.7795	27.51/0.7340	25.95/0.7808	**0.8774**	**15.1935**
	blm1-e[rb]	511	98.4	31.98/0.8921	28.45/0.7778	27.47/0.7328	25.80/0.7754	0.5456	*9.4559*
	blrn-e(r=2)[rg+u]	424	50	31.84/0.8898	28.34/0.7750	27.38/0.7295	25.52/0.7673	*0.6577*	5.6154
	blm1-e[rg]	413	92.8	32.02/0.8921	28.44/0.7765	27.44/0.7310	25.67/0.7715	0.5272	9.1481
	blrn-e(r=2)[rg]	612	104.3	32.02/0.8925	28.47/0.7779	27.48/0.7323	25.79/0.7755	0.5032	8.7419
	blm1-e[rg+u]	156	18.7	31.47/0.8847	28.12/0.7697	27.26/0.7252	25.16/0.7538	0.4928	4.211

worse. Regardless, our techniques can be applied to any model for further trade-offs between performance and efficiency.

Although our main objective is not to beat previous models but to understand and recommend techniques that can be applied to any existing model, we manage to derive models that are better or comparable to other models in the literature. For instance, in terms of size and evaluation metric, our best model (*blrn-e[rb]*) outperforms all models that have a count of 1,500K parameters and below. By comparing compute and evaluation, our best model performs better and has roughly x6 less operations than MemNet (Tai et al., 2017b). It is also comparable with the CARN model in the number of operations, trading a slightly worse performance with a 2.5x size reduction. Overall, our best model is better than earlier models such as VDSR (Kim et al., 2015b) and later models such as SRMDNF (Zhang et al., 2017a) for 3x and 4x scales. Our second and third best models also outperform earlier models in performance with huge savings in the number of operations for 3x and 4x scales. Our results show that these techniques which are designed for image discriminative tasks can be effective in SR. Visual comparisons for some of these models can be found in the appendix.

5 Quantization and low-precision under super resolution

In our next set of experiments, we examine the viability of quantization and the use of extreme low-precision (ternary/binary) as mechanisms to reduce system resource for SR.

5.1 Integer quantization

Motivation: With the success of low precision on neural networks on classification problems, we aim to show initial understanding of applying 8-bits integer quantization on our baseline model as described in section 4.1. Moving from 32-bits to 8-bits will result in a 4x reduction in memory and allow support for low-power embedded devices.

Approach: We train the model in full precision and apply the quantization scheme in Tensorflow-Lite for integer-only arithmetic (Jacob et al., 2017) and retrain for an additional 5 epochs with the a learning rate of $5e-5$.

Results: Our results show that applying quantization lead to a slight evaluation loss in 2x scaling and a slight improvement in 4x scaling. Our results are similar to that of classification Jacob et al. (2017). Furthermore the results show that deep neural networks are robust to noise and perturbations caused by quantization. Therefore, we strongly recommend quantization especially on hardware that can further utilise its benefits.

Table 3: We extend the table that is provided by Ahn et al. (2018) and compared our best three models (in order). For fair comparisons, we do not include models that are much bigger or much smaller than our derived models.

Scale	Model	Params (K)	Mult-Adds (G)	Set5 PSNR/SSIM	Set14 PSNR/SSIM	B100 PSNR/SSIM	Urban100 PSNR/SSIM
	VDSR (Kim et al., 2015b)	665	612.6	37.53/0.9587	33.03/0.9124	31.90/0.8960	30.76/0.9140
	DRCN (Kim et al., 2015a)	1,774	9,788.7	37.63/0.9588	33.04/0.9118	31.85/0.8942	30.75/0.9133
	LapSRN (Lai et al., 2017)	813	29.9	37.52/0.9590	33.08/0.9130	31.80/0.8950	30.41/0.9100
	DRRN (Tai et al., 2017a)	297	6,796.9	37.74/0.9591	33.23/0.9136	32.05/0.8973	31.23/0.9188
	BTSRN (Fan et al., 2017)	410	207.7	37.75/-	33.20/-	32.05/-	31.63/-
	MemNet (Tai et al., 2017b)	677	623.9	37.78/0.9597	33.28/0.9142	32.08/0.8978	31.31/0.9195
	SelNet (Choi & Kim, 2017)	974	225.7	37.89/0.9598	33.61/0.9160	32.08/0.8984	-
2×	SRMDNF (Zhang et al., 2017a)	2218	513.6	37.79/0.9601	33.32/0.9159	32.05/0.8985	31.33/0.9204
	D-DBPN (Haris et al., 2018)	1,261	158.9	38.09/0.9600	33.85/0.9190	32.27/0.9000	32.55/0.9324
	CARN (Ahn et al., 2018)	1,592	222.8	37.76/0.9590	33.52/0.9166	32.09/0.8978	31.92/0.9256
	CARN-M (Ahn et al., 2018)	412	91.2	37.53/0.9583	33.26/0.9141	31.92/0.8960	31.23/0.9193
	blrn-e(r=2)[rb](ours)	**535**	**156.8**	**37.75/0.9596**	**33.30/0.9153**	**32.00/0.8973**	**31.48/0.9218**
	blm1-e[rb](ours)	**363**	**117**	**37.65/0.9592**	**33.19/0.9143**	**31.92/0.8964**	**31.13/0.9181**
	blm1-e[rg](ours)	**265**	**94.7**	**37.59/0.9590**	**33.12/0.9132**	**31.87/0.8959**	**30.91/0.9158**
	VDSR (Kim et al., 2015b)	665	612.6	33.66/0.9213	29.77/0.8314	28.82/0.7976	27.14/0.8279
	DRCN (Kim et al., 2015a)	1,774	9,788.7	33.82/0.9226	29.76/0.8311	28.80/0.7963	27.15/0.8276
	DRRN (Tai et al., 2017a)	297	6,796.9	34.03/0.9244	29.96/0.8349	28.95/0.8004	27.53/0.8378
	BTSRN (Fan et al., 2017)	410	176.2	34.03/-	29.90/-	28.97/-	27.75/-
	MemNet (Tai et al., 2017b)	677	623.9	34.09/0.9248	30.00/0.8350	28.96/0.8001	27.56/0.8376
3×	SelNet (Choi & Kim, 2017)	1,159	120.0	34.27/0.9257	30.30/0.8399	28.97/0.8025	-
	SRMDNF (Zhang et al., 2017a)	2,956	305.5	34.12/0.9254	30.04/0.8382	28.97/0.8225	27.570.8398
	CARN (Ahn et al., 2018)	1,592	118.8	34.29/0.9255	30.29/0.8407	29.06/0.8034	28.06/0.8493
	CARN-M (Ahn et al., 2018)	412	46.1	33.99/0.9236	30.08/0.8367	28.91/0.8000	27.55/0.8385
	blrn-e(r=2)[rb](ours)	**609**	**108.1**	**34.19/0.9257**	**30.18/0.8394**	**29.00/0.8026**	**27.89/0.8469**
	blm1-e[rb](ours)	**437**	**90.5**	**34.09/0.9249**	**30.13/0.8379**	**28.95/0.8015**	**27.69/0.8419**
	blrn-e(r=2)[rg+u](ours)	**397**	**57.6**	**33.97/0.9236**	**30.04/0.8362**	**28.89/0.7997**	**27.50/0.8376**
	VDSR (Kim et al., 2015b)	665	612.6	31.35/0.8838	28.01/0.7674	27.29/0.7251	25.18/0.7524
	DRCN (Kim et al., 2015a)	1,774	9,788.7	31.53/0.8854	28.02/0.7670	27.23/0.7233	25.14/0.7510
	LapSRN (Lai et al., 2017)	813	149.4	31.54/0.8850	28.19/0.7720	27.32/0.7280	25.21/0.7560
	DRRN (Tai et al., 2017a)	297	6,796.9	31.68/0.8888	28.21/0.7720	27.38/0.7284	25.44/0.7638
	BTSRN (Fan et al., 2017)	410	165.2	31.85/-	28.20/-	27.47/-	25.74/-
	MemNet (Tai et al., 2017b)	677	623.9	31.74/0.8893	28.26/0.7723	27.40/0.7281	25.50/0.7630
	SelNet (Choi & Kim, 2017)	1,417	83.1	32.00/0.8931	28.49/0.7783	27.44/0.7325	-
4×	SRDenseNet (Tong et al., 2017)	2,015	389.9	32.02/0.8934	28.50/0.7782	27.53/0.7337	26.05/0.7819
	SRMDNF (Zhang et al., 2017a)	3,988	232.7	31.96/0.8925	28.35/0.7787	27.49/0.7337	25.68/0.7731
	D-DBPN (Haris et al., 2018)	2,207	79.7	32.47 0.8980	28.82/0.7860	27.72/0.7400	26.38/0.7946
	CARN (Ahn et al., 2018)	1,592	90.9	32.13/0.8937	28.60/0.7806	27.58/0.7349	26.07/0.7837
	CARN-M (Ahn et al., 2018)	412	32.5	31.92/0.8903	28.42/0.7762	27.44/0.7304	25.62/0.7694
	blrn-e(r=2)[rb](ours)	**683**	**108.3**	**32.10/0.8938**	**28.51/0.7795**	**27.51/0.7340**	**25.95/0.7808**
	blm1-e[rb](ours)	**511**	**98.4**	**31.98/0.8921**	**28.45/0.7778**	**27.47/0.7328**	**25.80/0.7754**
	blrn-e(r=2)[rg+u](ours)	**424**	**50**	**31.84/0.8898**	**28.34/0.7750**	**27.38/0.7295**	**25.52/0.7673**

Table 4: Quantitative results of applying 8-bit integer quantization in TF-Lite.

Scale	Model	Params (K)	Mult-Adds (G)	Set5 PSNR/SSIM	Set14 PSNR/SSIM	B100 PSNR/SSIM	Urban100 PSNR/SSIM
2×	bl	961	231.2	37.82/0.9599	33.36/0.9160	32.05/0.8981	31.67/0.9237
	bl_q			37.68/0.9582	33.34/0.9146	32.01/0.8966	31.64/0.9226
3×	bl	1191	122.4	34.20/0.9257	30.15/0.8392	29.01/0.8028	27.91/0.8467
	bl_q			34.17/0.9259	30.13/0.8393	29.00/0.8030	27.92/0.8474
4×	bl	1154	93	32.01/0.8927	28.41/0.7793	27.49/0.7337	25.87/0.7792
	bl_q			31.99/0.8922	28.43/0.7794	27.51/0.7337	25.88/0.7790

5.2 Ternary precision

Motivation: The success of using binarized (Courbariaux & Bengio, 2016; Rastegari et al., 2016; Lin et al., 2017) and ternarized neural networks (Li & Liu, 2016; Tschannen et al., 2017) to approximate the full-precision convolutions in image discriminative tasks motivates us to experiment the effectiveness of these techniques in SR.

Approach: We adapt the baseline SR architecture used in prior experiments in section 4.1 but modify it structurally by replacing every convolution layer with sum-product convolution layers proposed in StrassenNets (Tschannen et al., 2017). These sum-product convolution layers represent a sum-product network (SPN) that is used to approximate a matrix multiplication. Specifically, each convolution layer is replaced with a convolution layer that outputs r feature maps, followed by a element-wise multiplication and a transpose convolution layer. As both the convolution layers hold ternary weights, the number of multiply operations required is determined by the number of element-wise multiplication which is controlled by r. Besides outlining the trade-off of tuning r, we aggressively use group convolutions.

Results: Similar to section 5.1, the results in Table 5 are similar to that of image discriminative tasks. Specifically, the higher the width of the hidden layer of the SPN, r, the better the performance at a cost of additional multiplications and additions. When $r = 6c\_out$, we achieve an evaluation score that is close to the uncompressed model for 2x scales and suffer a slight drop for 3x and 4x scales. Any further attempts to increase r do not improve evaluation metric.

As proposed by Tschannen et al. (2017), we use group convolutions to reduce the number of additions. We take a step further and experiment with a wide range of groups as well. We found that the reduced number of additions do not justify the evaluation drop; the use of a lower r is better than the use of groups. Additionally, since multipliers are more costly and take up more area on chip than adders, we suggest lowering r instead of using grouped convolutions.

Table 5: Quantitative results of applying ternary-weighted SP convolutions. We omit the use of group convolutions as it leads to worse results. c_out refers to the number of output channels in each SP convolution layer.

Scale	Model	r	Reduction in Mult (%)	Reduction in Add (%)	Set5 PSNR/SSIM	Set14 PSNR/SSIM	B100 PSNR/SSIM	Urban100 PSNR/SSIM
2×	bl	-	-	-	37.86/0.9600	33.39/0.9159	32.06/0.8982	31.74/0.9248
	ST-bl	c_out	99.82	-15.96	37.59/0.9588	33.14/0.9138	31.88/0.8959	31.02/0.9171
		2c_out	99.64	-132.1	37.73/0.9595	33.30/0.9152	31.98/0.8973	31.37/0.9210
		4c_out	99.28	-364.38	37.81/0.9598	33.31/0.9151	32.03/0.8978	31.59/0.9229
		6c_out	98.92	-596.65	37.85/0.9600	33.41/0.9162	32.06/0.8981	31.68/0.9240
3×	bl	-	-	-	34.24/0.9260	30.26/0.8405	29.03/0.8033	27.96/0.8479
	ST-bl	c_out	99.81	-35.58	33.79/0.9215	29.92/0.8340	28.82/0.7983	27.25/0.8318
		2c_out	99.64	-171.33	33.99/0.9236	30.07/0.8365	28.91/0.8005	27.54/0.8389
		4c_out	99.28	-442.83	34.16/0.9250	30.11/0.8380	28.97/0.8021	27.73/0.8435
		6c_out	98.92	-714.33	34.17/0.9253	30.15/0.8383	28.99/0.8023	27.83/0.8454
4×	bl	-	-	-	32.06/0.8930	28.49/0.7787	27.50/0.7337	25.87/0.7788
	ST-bl	c_out	99.81	-26.04	31.46/0.8829	28.15/0.7709	27.27/0.7265	25.24/0.7566
		2c_out	99.64	-152.24	31.72/0.8871	28.31/0.7743	27.37/0.7296	25.49/0.7662
		4c_out	99.28	-404.65	31.90/0.8901	28.40/0.7770	27.45/0.7319	25.67/0.7723
		6c_out	98.93	-657.06	31.95/0.8907	28.43/0.7777	27.46/0.7324	25.77/0.7752

6 Best practices for efficient super-resolution

Through an extensive set of experiments, we show that some of the previous efficiency techniques that are successful in image discriminative tasks can be successfully applied to SR. Although these techniques are comparable in the former tasks, we highlight their varying effectiveness in SR and derive a list of best practices to construct or reduce any model that are designed to reduce image distortion:

- The sole use of low rank tensor decomposition (bottleneck design) results in the best trade-offs between performance and efficiency. If further compression of memory and/or compute is needed, separable/grouped convolution is recommended. If efficiency on conventional hardware is the topmost priority, we recommend reducing the number of layers or adopting the use of both channel splitting and shuffling (Ma et al., 2018).
- The fewer resource-efficient architecture changes applied, the better the trade-off. Therefore, we recommend a mixture of convolution and resource-efficient units unless further compression is needed.
- Avoid architecture changes on the first and last convolution layers.
- We strongly recommend using any form of quantization if the hardware supports it.

REFERENCES

Namhyuk Ahn, Byungkon Kang, and Kyung-Ah Sohn. Fast, accurate, and, lightweight super-resolution with cascading residual network. *CoRR*, abs/1803.08664, 2018. URL http://arxiv.org/abs/1803.08664.

Dzmitry Bahdanau, Kyunghyun Cho, and Yoshua Bengio. Neural machine translation by jointly learning to align and translate. *CoRR*, abs/1409.0473, 2014.

Marco Bevilacqua, Aline Roumy, Christine Guillemot, and Marie line Alberi Morel. Low-complexity single-image super-resolution based on nonnegative neighbor embedding. In *Proceedings of the British Machine Vision Conference*, pp. 135.1–135.10. BMVA Press, 2012. ISBN 1-901725-46-4. doi: http://dx.doi.org/10.5244/C.26.135.

Sourav Bhattacharya and Nicholas D. Lane. Sparsification and separation of deep learning layers for constrained resource inference on wearables. In *SenSys*, 2016.

Y. Blau, R. Mechrez, R. Timofte, T. Michaeli, and L. Zelnik-Manor. 2018 PIRM Challenge on Perceptual Image Super-resolution. *ArXiv e-prints*, September 2018.

Yochai Blau and Tomer Michaeli. The perception-distortion tradeoff. *CoRR*, abs/1711.06077, 2017.

Hong Chang, Dit-Yan Yeung, and Yimin Xiong. Super-resolution through neighbor embedding. *Proceedings of the 2004 IEEE Computer Society Conference on Computer Vision and Pattern Recognition, 2004. CVPR 2004.*, 1:I–I, 2004.

J.-H. Choi, J.-H. Kim, M. Cheon, and J.-S. Lee. Deep Learning-based Image Super-Resolution Considering Quantitative and Perceptual Quality. *ArXiv e-prints*, September 2018.

Jae-Seok Choi and Munchurl Kim. A deep convolutional neural network with selection units for super-resolution. In *The IEEE Conference on Computer Vision and Pattern Recognition (CVPR) Workshops*, July 2017.

Matthieu Courbariaux and Yoshua Bengio. Binarynet: Training deep neural networks with weights and activations constrained to +1 or -1. *CoRR*, abs/1602.02830, 2016.

Chao Dong, Chen Change Loy, Kaiming He, and Xiaoou Tang. Image super-resolution using deep convolutional networks. *CoRR*, abs/1501.00092, 2015. URL http://arxiv.org/abs/1501.00092.

Chao Dong, Chen Change Loy, and Xiaoou Tang. Accelerating the super-resolution convolutional neural network. *CoRR*, abs/1608.00367, 2016. URL http://arxiv.org/abs/1608.00367.

Yuchen Fan, Honghui Shi, Jiahui Yu, Ding Liu, Wei Han, Haichao Yu, Zhangyang Wang, Xinchao Wang, and Thomas S. Huang. Balanced two-stage residual networks for image super-resolution. *2017 IEEE Conference on Computer Vision and Pattern Recognition Workshops (CVPRW)*, pp. 1157–1164, 2017.

Ido Freeman, Lutz Roese-Koerner, and Anton Kummert. Effnet: An efficient structure for convolutional neural networks. *CoRR*, abs/1801.06434, 2018. URL http://arxiv.org/abs/1801.06434.

Leon A. Gatys, Alexander S. Ecker, and Matthias Bethge. Texture synthesis and the controlled generation of natural stimuli using convolutional neural networks. *CoRR*, abs/1505.07376, 2015.

Ian Goodfellow, Jean Pouget-Abadie, Mehdi Mirza, Bing Xu, David Warde-Farley, Sherjil Ozair, Aaron Courville, and Yoshua Bengio. Generative adversarial nets. In Z. Ghahramani, M. Welling, C. Cortes, N. D. Lawrence, and K. Q. Weinberger (eds.), *Advances in Neural Information Processing Systems 27*, pp. 2672–2680. Curran Associates, Inc., 2014. URL http://papers.nips.cc/paper/5423-generative-adversarial-nets.pdf.

S. Gu, R. Timofte, and L. Van Gool. Multi-bin Trainable Linear Unit for Fast Image Restoration Networks. *ArXiv e-prints*, July 2018.

Muhammad Haris, Greg Shakhnarovich, and Norimichi Ukita. Deep back-projection networks for super-resolution. *CoRR*, abs/1803.02735, 2018. URL `http://arxiv.org/abs/1803.02735`.

Kaiming He, Xiangyu Zhang, Shaoqing Ren, and Jian Sun. Deep residual learning for image recognition. *CoRR*, abs/1512.03385, 2015. URL `http://arxiv.org/abs/1512.03385`.

Andrew G. Howard, Menglong Zhu, Bo Chen, Dmitry Kalenichenko, Weijun Wang, Tobias Weyand, Marco Andreetto, and Hartwig Adam. Mobilenets: Efficient convolutional neural networks for mobile vision applications. *CoRR*, abs/1704.04861, 2017. URL `http://arxiv.org/abs/1704.04861`.

Gao Huang, Zhuang Liu, and Kilian Q. Weinberger. Densely connected convolutional networks. *CoRR*, abs/1608.06993, 2016.

J. Huang, A. Singh, and N. Ahuja. Single image super-resolution from transformed self-exemplars. In *2015 IEEE Conference on Computer Vision and Pattern Recognition (CVPR)*, pp. 5197–5206, June 2015. doi: 10.1109/CVPR.2015.7299156.

A. Ignatov, R. Timofte, T. Van Vu, T. M. Luu, T. X Pham, C. Van Nguyen, Y. Kim, J.-S. Choi, M. Kim, J. Huang, J. Ran, C. Xing, X. Zhou, P. Zhu, M. Geng, Y. Li, E. Agustsson, S. Gu, L. Van Gool, E. de Stoutz, N. Kobyshev, K. Nie, Y. Zhao, G. Li, T. Tong, Q. Gao, L. Hanwen, P. Navarrete Michelini, Z. Dan, H. Fengshuo, Z. Hui, X. Wang, L. Deng, R. Meng, J. Qin, Y. Shi, W. Wen, L. Lin, R. Feng, S. Wu, C. Dong, Y. Qiao, S. Vasu, N. Thekke Madam, P. Kandula, A. N. Rajagopalan, J. Liu, and C. Jung. PIRM Challenge on Perceptual Image Enhancement on Smartphones: Report. *ArXiv e-prints*, October 2018.

Benoit Jacob, Skirmantas Kligys, Bo Chen, Menglong Zhu, Matthew Tang, Andrew G. Howard, Hartwig Adam, and Dmitry Kalenichenko. Quantization and training of neural networks for efficient integer-arithmetic-only inference. *CoRR*, abs/1712.05877, 2017. URL `http://arxiv.org/abs/1712.05877`.

Luke Jaffe, Shiv Sundram, and Christian Martinez-Nieves. Super-resolution to improve classification accuracy of low-resolution images. Technical report, Tech. Rep. 19, Stanford University, 2017.

Justin Johnson, Alexandre Alahi, and Fei-Fei Li. Perceptual losses for real-time style transfer and super-resolution. *CoRR*, abs/1603.08155, 2016.

Jiwon Kim, Jung Kwon Lee, and Kyoung Mu Lee. Deeply-recursive convolutional network for image super-resolution. *CoRR*, abs/1511.04491, 2015a.

Jiwon Kim, Jung Kwon Lee, and Kyoung Mu Lee. Accurate image super-resolution using very deep convolutional networks. *CoRR*, abs/1511.04587, 2015b. URL `http://arxiv.org/abs/1511.04587`.

Jun-Hyuk Kim and Jong-Seok Lee. Deep residual network with enhanced upscaling module for super-resolution. In *The IEEE Conference on Computer Vision and Pattern Recognition (CVPR) Workshops*, June 2018.

Kwang In Kim and Younghee Kwon. Single-image super-resolution using sparse regression and natural image prior. *IEEE Trans. Pattern Anal. Mach. Intell.*, 32(6):1127–1133, 2010.

Yong-Deok Kim, Eunhyeok Park, Sungjoo Yoo, Taelim Choi, Lu Yang, and Dongjun Shin. Compression of deep convolutional neural networks for fast and low power mobile applications. *CoRR*, abs/1511.06530, 2015c.

Diederik P. Kingma and Jimmy Ba. Adam: A method for stochastic optimization. *CoRR*, abs/1412.6980, 2014. URL `http://arxiv.org/abs/1412.6980`.

Alex Krizhevsky, Ilya Sutskever, and Geoffrey E Hinton. Imagenet classification with deep convolutional neural networks. In F. Pereira, C. J. C. Burges, L. Bottou, and K. Q. Weinberger (eds.), *Advances in Neural Information Processing Systems 25*, pp. 1097–1105. Curran Associates, Inc., 2012. URL http://papers.nips.cc/paper/4824-imagenet-classification-with-deep-convolutional-neural-networks.pdf.

Wei-Sheng Lai, Jia-Bin Huang, Narendra Ahuja, and Ming-Hsuan Yang. Deep laplacian pyramid networks for fast and accurate super-resolution. *CoRR*, abs/1704.03915, 2017. URL http://arxiv.org/abs/1704.03915.

Christian Ledig, Lucas Theis, Ferenc Huszar, Jose Caballero, Andrew P. Aitken, Alykhan Tejani, Johannes Totz, Zehan Wang, and Wenzhe Shi. Photo-realistic single image super-resolution using a generative adversarial network. *CoRR*, abs/1609.04802, 2016.

Fengfu Li and Bin Liu. Ternary weight networks. *CoRR*, abs/1605.04711, 2016.

Bee Lim, Sanghyun Son, Heewon Kim, Seungjun Nah, and Kyoung Mu Lee. Enhanced deep residual networks for single image super-resolution. *CoRR*, abs/1707.02921, 2017. URL http://arxiv.org/abs/1707.02921.

Xiaofan Lin, Cong Zhao, and Wei Pan. Towards accurate binary convolutional neural network. *CoRR*, abs/1711.11294, 2017.

Yuan Liu, Yuancheng Wang, Nan Li, Xu Cheng, Yifeng Zhang, Yongming Huang, and Guojun Lu. An attention-based approach for single image super resolution. *CoRR*, abs/1807.06779, 2018.

Chao Ma, Chih-Yuan Yang, Xiaokang Yang, and Ming-Hsuan Yang. Learning a no-reference quality metric for single-image super-resolution. *CoRR*, abs/1612.05890, 2016.

N. Ma, X. Zhang, H.-T. Zheng, and J. Sun. ShuffleNet V2: Practical Guidelines for Efficient CNN Architecture Design. *ArXiv e-prints*, July 2018.

D. Martin, C. Fowlkes, D. Tal, and J. Malik. A database of human segmented natural images and its application to evaluating segmentation algorithms and measuring ecological statistics. In *Proceedings Eighth IEEE International Conference on Computer Vision. ICCV 2001*, volume 2, pp. 416–423 vol.2, July 2001. doi: 10.1109/ICCV.2001.937655.

Roey Mechrez, Itamar Talmi, Firas Shama, and Lihi Zelnik-Manor. Learning to maintain natural image statistics. *CoRR*, abs/1803.04626, 2018a.

Roey Mechrez, Itamar Talmi, and Lihi Zelnik-Manor. The contextual loss for image transformation with non-aligned data. *CoRR*, abs/1803.02077, 2018b.

Anish Mittal, Anush Krishna Moorthy, and Alan Conrad Bovik. No-reference image quality assessment in the spatial domain. *Trans. Img. Proc.*, 21(12):4695–4708, December 2012. ISSN 1057-7149. doi: 10.1109/TIP.2012.2214050. URL https://doi.org/10.1109/TIP.2012.2214050.

Anish Mittal, Rajiv Soundararajan, and Alan C. Bovik. Making a completely blind image quality analyzer. *IEEE Signal Processing Letters*, 20:209–212, 2013.

P. Navarrete Michelini, H. Liu, and D. Zhu. Mutigrid Backprojection Super-Resolution and Deep Filter Visualization. *ArXiv e-prints*, September 2018.

Mohammad Rastegari, Vicente Ordonez, Joseph Redmon, and Ali Farhadi. Xnor-net: Imagenet classification using binary convolutional neural networks. *CoRR*, abs/1603.05279, 2016.

Mark Sandler, Andrew G. Howard, Menglong Zhu, Andrey Zhmoginov, and Liang-Chieh Chen. Inverted residuals and linear bottlenecks: Mobile networks for classification, detection and segmentation. *CoRR*, abs/1801.04381, 2018. URL http://arxiv.org/abs/1801.04381.

H. R. Sheikh, A. C. Bovik, and G. de Veciana. An information fidelity criterion for image quality assessment using natural scene statistics. *IEEE Transactions on Image Processing*, 14:2117–2128, December 2005. doi: 10.1109/TIP.2005.859389.

Ying Tai, Jian Yang, and Xiaoming Liu. Image super-resolution via deep recursive residual network. In *Proceedings of the IEEE Conference on Computer Vision and Pattern Recognition*, 2017a.

Ying Tai, Jian Yang, Xiaoming Liu, and Chunyan Xu. Memnet: A persistent memory network for image restoration. *CoRR*, abs/1708.02209, 2017b.

R. Timofte, E. Agustsson, L. V. Gool, M. Yang, L. Zhang, B. Lim, S. Son, H. Kim, S. Nah, K. M. Lee, X. Wang, Y. Tian, K. Yu, Y. Zhang, S. Wu, C. Dong, L. Lin, Y. Qiao, C. C. Loy, W. Bae, J. Yoo, Y. Han, J. C. Ye, J. Choi, M. Kim, Y. Fan, J. Yu, W. Han, D. Liu, H. Yu, Z. Wang, H. Shi, X. Wang, T. S. Huang, Y. Chen, K. Zhang, W. Zuo, Z. Tang, L. Luo, S. Li, M. Fu, L. Cao, W. Heng, G. Bui, T. Le, Y. Duan, D. Tao, R. Wang, X. Lin, J. Pang, J. Xu, Y. Zhao, X. Xu, J. Pan, D. Sun, Y. Zhang, X. Song, Y. Dai, X. Qin, X. Huynh, T. Guo, H. S. Mousavi, T. H. Vu, V. Monga, C. Cruz, K. Egiazarian, V. Katkovnik, R. Mehta, A. K. Jain, A. Agarwalla, C. V. S. Praveen, R. Zhou, H. Wen, C. Zhu, Z. Xia, Z. Wang, and Q. Guo. Ntire 2017 challenge on single image super-resolution: Methods and results. In *2017 IEEE Conference on Computer Vision and Pattern Recognition Workshops (CVPRW)*, pp. 1110–1121, July 2017. doi: 10.1109/CVPRW.2017.149.

Radu Timofte, Vincent De Smet, and Luc J. Van Gool. Anchored neighborhood regression for fast example-based super-resolution. In *ICCV*, pp. 1920–1927. IEEE Computer Society, 2013.

Tong Tong, Gen Li, Xiejie Liu, and Qinquan Gao. Image super-resolution using dense skip connections. *2017 IEEE International Conference on Computer Vision (ICCV)*, pp. 4809–4817, 2017.

Michael Tschannen, Aran Khanna, and Anima Anandkumar. Strassennets: Deep learning with a multiplication budget. *CoRR*, abs/1712.03942, 2017. URL `http://arxiv.org/abs/1712.03942`.

X. Wang, K. Yu, S. Wu, J. Gu, Y. Liu, C. Dong, C. Change Loy, Y. Qiao, and X. Tang. ESRGAN: Enhanced Super-Resolution Generative Adversarial Networks. *ArXiv e-prints*, September 2018.

Zhou Wang, A. C. Bovik, H. R. Sheikh, and E. P. Simoncelli. Image quality assessment: From error visibility to structural similarity. *Trans. Img. Proc.*, 13(4):600–612, April 2004. ISSN 1057-7149. doi: 10.1109/TIP.2003.819861. URL `http://dx.doi.org/10.1109/TIP.2003.819861`.

Saining Xie, Ross B. Girshick, Piotr Dollár, Zhuowen Tu, and Kaiming He. Aggregated residual transformations for deep neural networks. *CoRR*, abs/1611.05431, 2016. URL `http://arxiv.org/abs/1611.05431`.

Jianchao Yang, John Wright, Thomas S. Huang, and Yi Ma. Image super-resolution via sparse representation. *Trans. Img. Proc.*, 19(11):2861–2873, November 2010. ISSN 1057-7149. doi: 10.1109/TIP.2010.2050625. URL `http://dx.doi.org/10.1109/TIP.2010.2050625`.

Dong-Qing Zhang. clcnet: Improving the efficiency of convolutional neural network using channel local convolutions. *CoRR*, abs/1712.06145, 2017. URL `http://arxiv.org/abs/1712.06145`.

Kai Zhang, Wangmeng Zuo, and Lei Zhang. Learning a single convolutional super-resolution network for multiple degradations. *CoRR*, abs/1712.06116, 2017a. URL `http://arxiv.org/abs/1712.06116`.

Xiangyu Zhang, Xinyu Zhou, Mengxiao Lin, and Jian Sun. Shufflenet: An extremely efficient convolutional neural network for mobile devices. *CoRR*, abs/1707.01083, 2017b. URL `http://arxiv.org/abs/1707.01083`.

Y. Zhang, K. Li, K. Li, L. Wang, B. Zhong, and Y. Fu. Image Super-Resolution Using Very Deep Residual Channel Attention Networks. *ArXiv e-prints*, July 2018.

Yulun Zhang, Yapeng Tian, Yu Kong, Bineng Zhong, and Yun Fu. Residual dense network for image super-resolution. *CoRR*, abs/1802.08797, 2018. URL `http://arxiv.org/abs/1802.08797`.

A VISUAL COMPARISON ON X4 SCALE BENCHMARKS

HR (PSNR/SSIM) RCAN (29.35/0.9342) VDSR (26.92/0.8956)

LapSRN (25.84/0.8722) blm1-e [rb] (28.29/0.9214) blrn-e[rb] (28.64/0.9255)

HR (PSNR/SSIM) RCAN (27.95/0.7910) VDSR (26.50/0.7525)

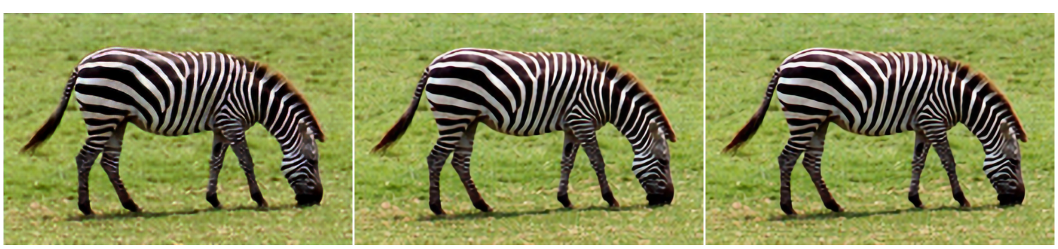

LapSRN (26.28/0.7562) blm1-e [rb] (27.19/0.7796) blrn-e[rb] (27.23/0.7802)

Figure 2: Visual comparisons with state-of-the-art models on *Set5* and *Set14*. VSDR and LapSRN are comparable to our models with regards to model size and/or number of operations and RCAN is x22.8-x30.5 larger and has x8.4-x9.3 more operations.

Figure 3: Visual comparisons with state-of-the-art models on *B100*.

HR (PSNR/SSIM) RCAN (27.95/0.8570) VDSR (25.61/0.7623)

LapSRN (25.76/0.7810) blm1-e [rb] (26.55/0.8124) blrn-e[rb] (26.70/0.8167)

HR (PSNR/SSIM) RCAN (28.02/0.8907) VDSR (24.93/0.7952)

LapSRN (25.17/0.8078) blm1-e [rb] (27.10/0.8680) blrn-e[rb] (27.14/0.8704)

Figure 4: Visual comparisons with state-of-the-art models on *Urban100*.

HR (PSNR/SSIM) | RCAN (23.45/0.6040) | VDSR (22.49/0.5454)

LapSRN (22.35/0.5494) | blm1-e [rb] (22.94/0.5790) | blrn-e[rb] (23.02/0.5836)

HR (PSNR/SSIM) | RCAN (27.96/0.8661) | VDSR (26.33/0.8045)

LapSRN (26.37/0.8166) | blm1-e [rb] (27.12/0.8395) | blrn-e[rb] (27.30/0.8444)

Figure 5: More x4 scale visual comparisons on *Urban100*